Remote Sensing of Environment 112 (2008) 2914–2926

Contents lists available at ScienceDirect

Remote Sensing of Environment

journal homepage: www.elsevier.com/locate/rse

North American forest disturbance mapped from a decadal Landsat record

Jeffrey G. Masek [a,*], Chengquan Huang [b], Robert Wolfe [a], Warren Cohen [c], Forrest Hall [d], Jonathan Kutler [a], Peder Nelson [c]

[a] Hydrospheric and Biospheric Sciences Laboratory, NASA Goddard Space Flight Center, Greenbelt, Maryland, USA
[b] Department of Geography, University of Maryland, College Park, Maryland, USA
[c] US Forest Service Pacific Northwest Research Station, Corvallis, Oregon, USA
[d] Joint Center for Earth Systems Technology, University of Maryland Baltimore County, Baltimore, Maryland, USA

ARTICLE INFO

Article history:
Received 26 December 2006
Received in revised form 8 February 2008
Accepted 9 February 2008

Keywords:
Remote sensing
Landsat
Change detection
Forestry
Disturbance

ABSTRACT

Forest disturbance and recovery are critical ecosystem processes, but the spatial pattern of disturbance has never been mapped across North America. The LEDAPS (Landsat Ecosystem Disturbance Adaptive Processing System) project has assembled a wall-to-wall record of stand-clearing disturbance (clearcut harvest, fire) for the United States and Canada for the period 1990–2000 using the Landsat satellite archive. Landsat TM and ETM+ data were first converted to surface reflectance using the MODIS/6S atmospheric correction approach. Disturbance and early recovery were mapped using the temporal change in a Tasseled-Cap "Disturbance Index" calculated from the early (~1990) and later (~2000) images. Validation of the continental mapping has been carried out using a sample of biennial Landsat time series from 23 locations across the United States. Although a significant amount of disturbance (30–60%) cannot be mapped due to the long interval between image acquisition dates, the biennial analyses allow a first-order correction of the decadal mapping. Our results indicate disturbance rates of up to 2–3% per year are common across the US and Canada due primarily to harvest and forest fire. Rates are highest in the southeastern US, the Pacific Northwest, Maine, and Quebec. The mean disturbance rate for the conterminous United States (the "lower 48" states and District of Columbia) is calculated as 0.9 +/−0.2% per year, corresponding to a turnover period of 110 years.

1. Introduction

Forest disturbance and recovery have been regarded as critical, but poorly quantified, mechanisms for transferring carbon between the land surface and the atmosphere. (Houghton, 1999; Pacala et al., 2001). Disturbance events (fires, harvest) emit carbon to the atmosphere through oxidation and decomposition of wood. Conversely, recovery from past disturbance tends to sequester carbon from the atmosphere since young forests can be highly productive and have lower levels of heterotrophic respiration (Barford et al., 2001; Odum, 1969; Thornton et al., 2002). The balance of these processes across the landscape is one control on overall (net) ecosystem productivity.

The uncertainties associated with the North American carbon cycle have led the United States Global Change Research Program (USGCRP) to organize the North American Carbon Program (NACP–Wofsy & Harriss, 2002), an integrated program of satellite, aircraft and ground measurements and modeling to estimate the magnitude of North American carbon fluxes and understand the underlying processes. Although the US Forest Service (USFS) Forest Inventory and Analysis (FIA) program tracks forest extent and condition through a network of plots (Reams et al., 2005), these measurements are neither sufficiently dense nor consistent enough through time to map local changes in forest structure. Given the uncertainties in the land-cover carbon fluxes, the science plan for the NACP has specified the need for satellite-based estimates of U.S. disturbance and recovery, and land-use and land-cover change, which could improve the accuracy of and periodically update the USFS ground-based estimates (Wofsy & Harriss, 2002). The Canadian Forest Service provides annual estimates of Canada's net forest carbon flux through the Carbon Budget Model for the Canadian Forest Sector (CBM-CFS2) model (Kurz & Apps, 1999), including the effects of disturbance and harvest on carbon balances. While the need for satellite-based disturbance estimates is thus less pressing for Canada, establishing a consistent, continent-wide synthesis of disturbance rates is of interest to the NACP.

The Landsat Ecosystem Disturbance Adaptive Processing System (LEDAPS) project has been funded by NASA to develop a robust system for processing large quantities of remote sensing data for forest change analysis. A major goal of this project is to produce wall-to-wall maps of stand-clearing forest disturbance and regrowth for the North American continent using a decadal (1990–2000) revisit period. The North American disturbance and regrowth data products developed through the LEDAPS project are primarily intended for the carbon modeling community. However, it is expected that ecologists, foresters, and remote sensing scientists will also find them of interest.

In this paper we describe the disturbance mapping algorithm, present validation results at a range of spatial scales, and show results for

* Corresponding author.
E-mail address: Jeffrey.G.Masek@nasa.gov (J.G. Masek).

0034-4257/$ – see front matter © 2008 Elsevier Inc. All rights reserved.
doi:10.1016/j.rse.2008.02.010

the United States and Canada. The data products discussed in this study are available for download from the NASA Goddard Space Flight Center.[1]

2. Disturbance mapping goals

The overall goal of the LEDAPS disturbance mapping has been to provide useful information on disturbance rates for carbon accounting and biogeochemical modeling. Ideally, we would be able to use historical remote sensing to determine both disturbance rates and their variability at high-resolution across North America, over the last 30–40 years (e.g. Cohen et al., 2002; Masek & Collatz, 2006). Assuming biennial coverage with Landsat data, and ~1100 scene centers across the continent, such an undertaking would require processing approximately 16,000 Landsat images. While processing this data volume is tractable with data processing systems such as EOSDIS, Landsat data costs precluded such an analysis for this study.[2] Instead we have relied on the decadal Landsat GeoCover data set with images from a 1990 and 2000-era epochs, described more fully in Section 3. Change detection (discussed below) was then used to isolate "disturbance" and "regrowth" classes from each 1990–2000 image pair.

The mapping effort was targeted toward detecting stand-clearing disturbance events (biomass loss, primarily from clearcuts and fires) and recovery (biomass gain). Disturbance events that leave intact substantial portions of the forest canopy, such as partial harvest, insect outbreaks, thinning, and storm damage, cannot be generally be mapped using the 10-year observation interval (e.g. Jin & Sader, 2005; Lunetta et al., 2004; Wulder et al., 2005). However, it is not always possible to distinguish older stand-clearing events from more recent non-clearing disturbance. For example, thinning that occurred immediately before the 2000 image acquisition could be readily confused with a recovering clearcut from the early 1990s.

We also note that mapping "regrowth" as a class is inherently problematic due to the gradual nature of biomass accumulation following disturbance. Biologically, most stands are regrowing from a past disturbance in the sense that they continue to add biomass. From a remote sensing perspective, the "regrowth" class only includes stands for which biomass accumulation is sufficiently rapid over 10 years to be detected in optical imagery. For example, while it might be possible to map a forest stand last cleared in the mid-1980's as "regrowth" using data from the 1990–2000 period, it is highly unlikely a stand cleared in the 1930's would be so mapped. Given this uncertainty, it is critical that any study identifying a "regrowth" class calibrate that class to a particular range of stand ages using other data sources.

In addition to maps of "disturbance" and "regrowth" classes at 28.5-meter resolution, we have also prepared a set of gridded products to support biogeochemical modeling. These products include 500-meter and 0.05 degree resolution maps recording the rate of disturbance or regrowth for each cell (% of cell area disturbed per year).

3. Data sources and preprocessing

The GeoCover data set is a global collection of orthorectified, mostly cloud-free Landsat imagery, centered on 1975, 1990, and 2000 epochs (Tucker et al., 2004). Actual image acquisition dates vary depending on data availability, but for North America most acquisitions date from 1986–1992 for the 1990-epoch coverage, and 1999–2001 for the 2000-epoch coverage (Table 1). In addition, not all images were acquired during peak-greenness conditions, and the 1990 and 2000 epoch data were not necessarily acquired during the same month.

The GeoCover data were orthorectified by Earth Satellite Corporation (now MDA Federal) using limited ground control and digital terrain from a variety of sources, including Digital Terrain Elevation Data (DTED) and GTOPO30 (Tucker et al., 2004). Within the United States, the National Elevation Dataset (NED) was used as the topographic reference. The absolute geodetic accuracy of the data set was specified at <50 m RMSE for multi-scene blocks. While the product did meet this specification, geodetic errors as high as ~200 m can occur for individual images in high-relief areas, or where geodetic control was particularly sparse (Jon Dykstra, personal communication). However, since the 2000 GeoCover data set was matched to the 1990, relative misregistration between the two epochs is generally very small. No cases of significant relative misregistration were found during LEDAPS processing or validation.

Table 1
Distribution of North American LEDAPS images by year (including GeoCover and supplementary images)

"1990" Epoch		"2000" Epoch	
1984	2	1999	225
1985	28	2000	428
1986	67	2001	379
1987	130	2002	182
1988	158		
1989	188		
1990	224		
1991	183		
1992	117		
1993	57		
1994	11		
1995	13		

For approximately 60 images, the GeoCover acquisition dates fell well outside of the growing season. These images were replaced by additional acquisitions from the USGS Landsat archive. These additional images were procured as UTM, Level 1G data, matched using the GeoCover 2000 image as geodetic control, and orthorectified using SRTM 90 m digital elevation data.

Data from the 1990 and 2000 epochs were calibrated and atmospherically corrected to surface reflectance using the MODIS 6S radiative transfer approach (Masek et al., 2006; Vermote et al., 1997). For Landsat-5, the original calibration derived from the on-board calibrator lamps was removed, and the newest calibration history applied (Chander et al., 2007; Masek et al., 2006). No bi-directional reflectance distribution function (BRDF) or topographic illumination correction was applied.

4. Disturbance Index algorithm

4.1. Algorithm description

To assess disturbance across ~1100 Landsat pairs, an automated mapping approach was required. Numerous studies have presented change detection approaches suitable for forest environments (see reviews by Coppin et al., 2004; Lu et al., 2004). Several considerations influenced the decision of which approach to take for the LEDAPS. Given the variations in acquisition date between images, the change detection methodology needed to be relatively insensitive to BRDF variability and phenology. This requirement highlighted approaches that use within-image statistics to normalize radiometric change. It was also desired to have a continuous metric related to gain or loss of biomass, rather than a "hard" classification. Finally, approaches that relied on the physical aspects of reflectance variations were preferred to approaches that relied exclusively on statistical generalization from training samples. While the purely statistical approach can produce excellent results in most cases, it is also susceptible to failure in cases where training data are insufficient or of poor quality. A relatively simple and flexible approach, the Disturbance Index (DI) of Healey et al. (2005) satisfied these criteria and was used for this study.

The DI is a transformation of the Landsat Tasseled-Cap data space (Crist & Cicone, 1984; Huang et al., 2002; Kauth & Thomas, 1976),

[1] http://ledaps.nascom.nasa.gov/ledaps/ledaps_NorthAmerica.html.
[2] In early 2008 USGS announced plans to make all Landsat TM and ETM+ data available at no cost by the end of 2009.

specifically designed for sensitivity to forest change. The Tasseled-Cap brightness, greenness, and wetness indices are a standard transformation of the original Landsat spectral bands, effectively capturing the three major axes of spectral variation across the solar reflective spectrum. Originally developed for use in agricultural systems, the Tasseled-Cap indices received increasing attention after the launch of the TM sensor in 1982, which included shortwave infrared (SWIR) bands. Horler and Ahern (1986) were among the first to explore the forestry information content TM data, discovering that SWIR bands were the most important for characterizing forest structure. As chronicled by Cohen and Goward (2004), this led to a resurgence of interest in the Tasseled-Cap, particularly the wetness index, which contrasts SWIR against near-infrared reflectance. Brightness, greenness, and wetness are now commonly used indices across a variety of forestry remote sensing applications (Cohen and Goward (2004), and has been extended to data from the Moderate Resolution Imaging Spectroradiometer (MODIS) for a broader set of uses (Lobser & Cohen, 2007).

At a basic level the DI records the normalized spectral distance of any given pixel from a nominal "mature forest" class to a "bare soil" class. The DI is calculated using the Tasseled-Cap (brightness–greenness–wetness) indices for Landsat TM/ETM+ (Crist & Cicone, 1984; Huang et al., 2002; Kauth & Thomas, 1976):

$$\mathrm{DI} = B' - (G' + W') \tag{1}$$

Where B', G', and W' represent the Tasseled-Cap brightness, greenness, and wetness indices normalized by a dense forest class for each Landsat scene, such that (for example):

$$B' = \frac{B - \mu_B}{\sigma_B} \tag{2}$$

where μ_B is the mean Tasseled-Cap brightness index of the dense forest class for a particular scene, and σ_B is the standard deviation of brightness within the dense forest class for a particular scene. Thus, the DI records

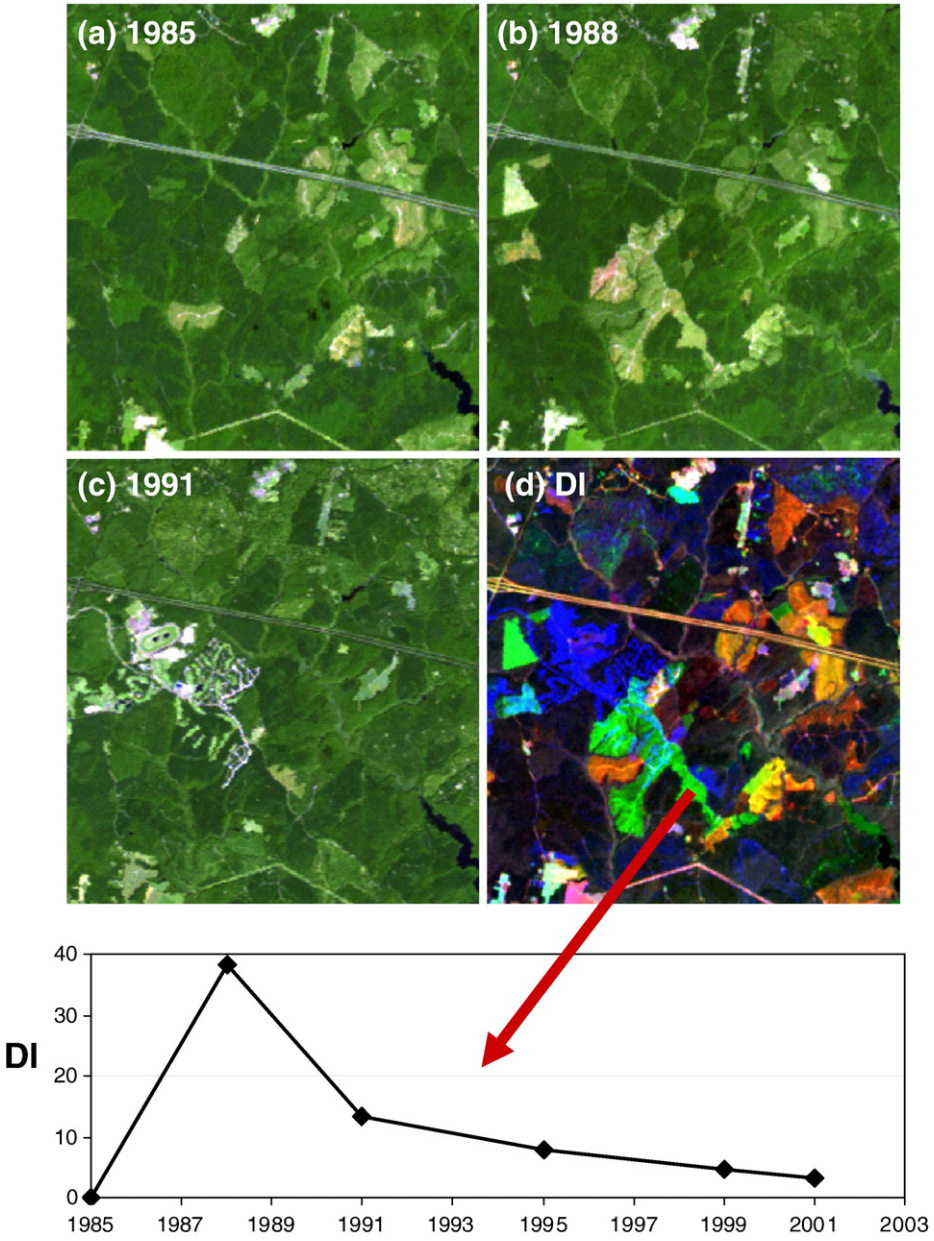

Fig. 1. Example of the Disturbance Index applied to a series of Landsat imagery from Central Virginia. (a)–(c): RGB images (753 band combination) from the same region from 1985, 1988, and 1991. (d) RGB composite created by assigning DI values from 1985, 1988, and 1999 to red, green, and blue, respectively. (bottom): chart showing the evolution of DI value for one patch disturbed during 1985–88.

the spectral distance of a given pixel from the dense forest "centroid" for that scene, in units of within-class standard deviation. DI values greater than ~1 have a high probability of being disturbed or non-forest. Since the DI values are based on the statistics of forest reflectance from individual scenes, the DI metric is relatively insensitive to variability in solar geometry or BRDF between scenes, and lessens the effect of vegetation phenologic variability among image dates. The LEDAPS process for automatically identifying sample "dense forest" targets for the normalization is discussed below. As demonstrated by Healey et al. (2005) the DI is a simple and effective means of tracking vegetation disturbance across a variety of forest ecosystems. Unlike simple visible/near-infrared indices (e.g. the Normalized Difference Vegetation Index or NDVI) the DI incorporates tasseled-Cap wetness, and hence information from the shortwave infrared, which is critical for assessing changes in forest structure (Cohen and Goward, 2004).

The original application by Healey et al. (2005) relied on the absolute value of the DI from individual scenes to assess disturbance extent. In contrast, the LEDAPS algorithm used the decadal change in DI value (ΔDI) as a more robust metric to identify disturbance and recovery. The use of ΔDI directly incorporates the magnitude of radiometric change between two images, screening out features far from the "dense forest" spectral feature, but which do not change through time. An example from a dense time series of Landsat imagery of central Virginia illustrates how the DI records planted pine harvest and recovery (Fig. 1).

This overall processing flow is illustrated in Fig. 2, beginning with the atmospheric correction of each scene to surface reflectance. Each subsequent step is described more fully below.

Step 1. Tasseled-Cap calculation. Tasseled-Cap (brightness, greenness, and wetness) images were calculated from the 1990 and 2000 surface reflectance images using the reflectance factor transform given in Crist (1985).

Step 2. Tasseled-Cap normalization To normalize the Tasseled-Cap images, a "dense forest" class was identified in the 2000 GeoCover TM/ETM+ images using the MODIS Vegetation Continuous Fields (VCF) product (Hansen et al., 2002), which includes estimates for the fraction of treecover (projection of tree crown area) at a resolution of 500 m. TM/ETM+ pixels with normalized difference vegetation index (NDVI)> NDVI_thresh and VCF treecover>VCF_thresh were identified as likely forest pixels. The corresponding 1990 mature forest class was that subset of the TM/ETM+ mature forest class that did not experience significant radiometric change (defined as a change in Tasseled-Cap brightness) between 1990 and 2000. Note that the normalization step occurred independently for each scene and tended to suppress the effects of scene-to-scene variability in overall reflectance due to small changes in BRDF or phenology.

Step 3. DI and ΔDI calculation. Given the population of mature forest pixels from step 2, the mean and standard deviation of each Tasseled-Cap component for the class were calculated. Each Tasseled-Cap image plane was then normalized as in Eqs. (1) and (2). The ΔDI was calculated as the temporal change DI2000–DI1990. Large positive values of ΔDI corresponded to likely disturbance events; large negative values corresponded to likely regrowth. Thresholds were applied to the ΔDI values to identify potential disturbance (ΔDI> ΔDI_dist_thresh) and regrowth (ΔDI<ΔDI_regr_thresh). A conditional second pass used a 5×5 pixel contextual window and less restrictive thresholds. If more than 20% of the pixels within the window were classified as potential disturbance/regrowth from Pass 1, the central pixel ΔDI value was tested against the less restrictive set of thresholds. The purpose of Pass 2 was to fill out patches of forest change that were incompletely mapped during the first pass.

An example of the disturbance mapping algorithm is shown for a small area of Washington State in Fig. 3. Recent clearcuts and logging roads are successfully identified, as are regions of recovery from past clearing. Table 2 gives sample parameter values used in classifying disturbance in the Mid-Atlantic ecoregion.

Step 4. Filtering non-forest change. Other land-cover transformations may be inadvertently identified by these ΔDI trends, particularly agricultural cropping patterns. We removed these artifacts by screening the map with a forest/non-forest mask. Initial attempts were made to use the 1992 MRLC National Land Cover Dataset (NLCD) (Vogelmann

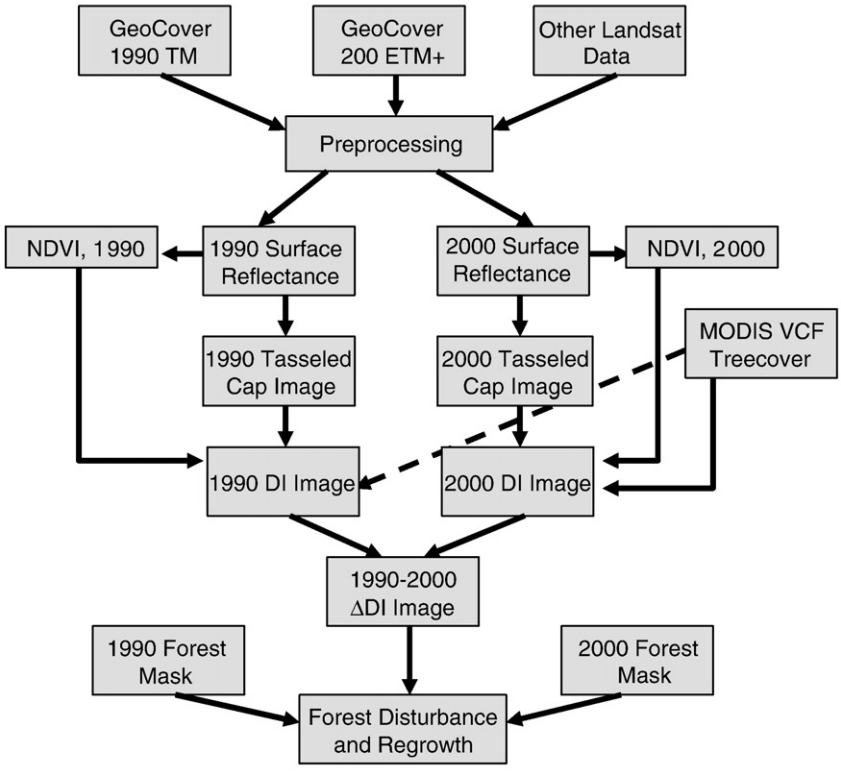

Fig. 2. Flow chart illustrating the LEDAPS disturbance/recovery mapping approach.

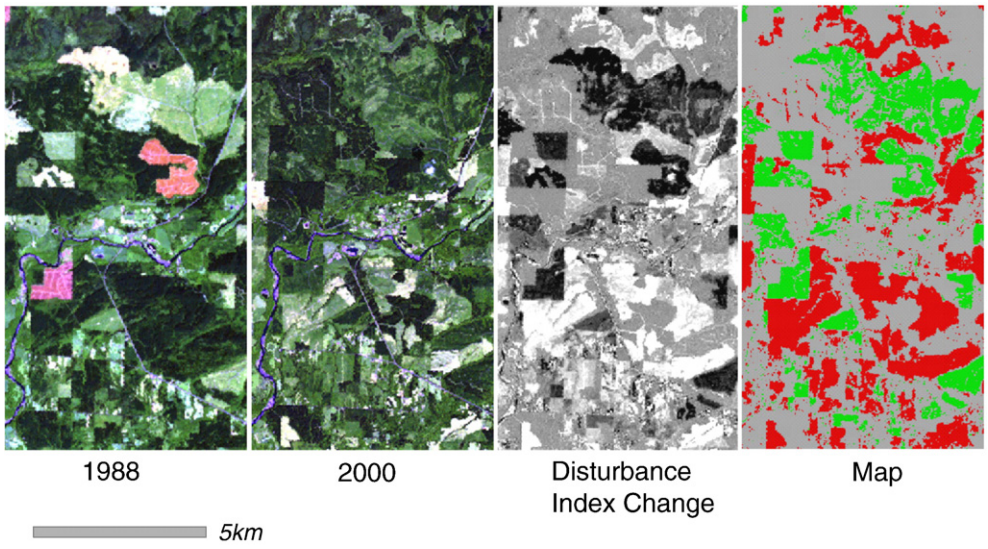

Fig. 3. Disturbance map from the Olympic Peninsula, Washington. (a) 1988 RGB Landsat image subset; (b) 2000 RGB Landsat image subset; (c) change in the Disturbance Index parameter; dark values correspond to decreasing DI values through time (regrowth), light values correspond to increasing DI values through time (disturbance); (d) disturbance (red) and regrowth (green) derived from (c) after thresholds were applied. Sieve filtering was not included in this example.

et al., 2001; Wickham et al., 2004) as the forest/non-forest mask, but disturbances occurring early in the 1990's often resulted in the NLCD identifying the patch as "non-forest". As a result, a forest/non-forest mask was produced independently for each image (1990 and 2000) using a "fuzzy classifier". The classifier blended three metrics indicative of forest cover: (1) the MODIS VCF treecover product; (2) the DI value itself; and (3) the ratio of red reflectance (ρ3) to NDVI (redNDVI). These metrics were transformed to independent estimates of probability of membership in the forest class (P) according to:

$$P_{\mathrm{VCF}} = \left\{ \begin{array}{c} 0 \text{ for VCF}<20\% \\ \mathrm{VCF}/\mathrm{VCF}_{\max} \text{ for VCF}>20\% \end{array} \right\} \quad (3)$$

$$P_{\mathrm{DI}} = e^{\frac{-(\alpha \mathrm{DI})^2}{2}} \quad (4)$$

$$P_{\mathrm{redNDVI}} \frac{1}{1 + e^{\nu\left(\frac{\rho 3}{\mathrm{NDVI}} + \eta\right)}} \quad (5)$$

where $\mathrm{VCF}_{\max}$ represents the local upperbound on treecover as recorded by the MODIS VCF product, and α, γ, and η are empirical scaling parameters used to scale the raw metrics (DI, redNDVI) for the Gaussian probability function (4) or sigmoid probability function (5). The overall probability of forest class membership (P_f) was calculated as a weighted sum of the three independent metrics:

$$P_f = w_{\mathrm{VCF}} P_{\mathrm{VCF}} + w_{\mathrm{DI}} P_{\mathrm{DI}} + w_{\mathrm{redNDVI}} P_{\mathrm{redNDVI}} \quad (6)$$

where the sum of the weighting factors (w) are constrained to unity. A high value of P_f (>~0.6) indicates that the pixel is likely to be forested. The classifier was not particularly sensitive to the exact threshold in P_f, since the vast majority of pixels tended to cluster at either very low or very high values of P_f. If either or both the circa-1990 and/or circa-2000 pixel was labeled as 'forest', then the pixel is retained in the disturbance/regrowth map. Table 3 gives sample parameter values for the forest/non-forest classification for the Mid-Atlantic ecoregion.

For some locations we used the 1992 MRLC National Land Cover Dataset (NLCD) as an additional screening. Wetlands may be confused with forest, and are susceptible to seasonal variations in water level that can be confused with disturbance. Pixels for which the 1992 NLCD classification is either "Forested wetland" or "Permanent Wetland" were screened from the disturbance map. Finally, in the southern Rocky Mountains, the fuzzy forest classifier did not prove reliable due to sparse canopy cover, topographic shadowing, and confusion with closed shrublands. For this region we used the NLCD directly to separate forest and non-forest land-cover. For the western United States the NLCD forest land users's accuracy ranges from 66–83% (depending on Federal Region), while the producer's accuracy ranges from 78–93%. (Wickham et al., 2004; see also revised figures given on http://landcover.usgs.gov/accuracy/index.php).

Step 5: Post-processing. Three final steps were implemented to finalize the disturbance map. First, a 5×5 pixel sieve filter is used to remove small patches of disturbance or recovery, including "speckle" associated with slight misregistration in the imagery. Given the GeoCover pixel resolution of 28.5 m, this filter also imposed a ~0.50 ha minimum-mapping area on the products. Second, a water mask (based on near-infrared reflectance) was calculated for each scene, and any water pixels were removed from the disturbance map. Finally,

Table 2
Sample parameters for the ΔDI disturbance classification, for the Mid-Atlantic Ecoregion

Parameter	Purpose	Value
NDVI_thresh	Minimum NDVI for obtaining forest population during Tasseled-Cap normalization	0.8
VCF_thresh	Minimum treecover percentage for obtaining forest population during Tasseled-Cap normalization	70%
ΔDI_dist_thresh	Threshold Disturbance Index change for assigning "disturbance" class	>0.8
ΔDI_regr_thresh	Threshold Disturbance Index change for assigning "regrowth" class	< −0.6

See Section 4.1 for discussion.

Table 3
Sample parameters for the "fuzzy" forest classification for the Mid-Atlantic Ecoregion

Parameter	Purpose	Value
$\mathrm{VCF}_{\max}$	Normalization for P_{VCF} component	100%
α	Scaling for P_{DI} component	0.10
ν	Scaling for P_{redNDVI} component	250.0
η	Scaling for P_{redNDVI} component	−0.04
w_{VCF}	Weight for P_{VCF} component	0.25
w_{DI}	Weight for P_{DI} component	1.0
w_{redNDVI}	Weight for P_{redNDVI} component	1.0

See Eqs. (3)–(6) for context.
Note that these parameters assume the LEDAPS convention for surface reflectance inputs (16-bit values scaled 0 to 10000 representing 0 to 100% reflectance).

the MODIS VCF treecover product was used to find areas with less than 10% treecover that are far (>5 km) from any area with greater than 10% treecover. These areas were screened from the final map. The intent of this final filter is to remove any disturbance signal from purely agricultural, rangeland, or desert landscapes. Even a very small commission error over a broad agricultural area could result in a significant overestimation of disturbed area. This "landscape scale" filter eliminated this risk.

4.2. Algorithm calibration

The DI algorithm requires multiple parameters that can be "tuned" for a particular geographic area. Within LEDAPS, we allowed separate processing parameters for each North American Commission for Environmental Cooperation (CEC) Level-2 Ecoregion (Commission for Environmental Cooperation, 1997). Although the tasseled-cap normalization (Step 2 above) occurred on a per-scene basis, the other processing parameters were adjusted only on a per-ecoregion basis. One exception was CEC Ecoregion 6.2 ("Western Cordillera") which extends from northern British Columbia to central New Mexico. The vast differences in tree type, size, and canopy cover between these extremes necessitated splitting the ecoregion near the southern border of Idaho. Several Landsat scenes from each ecoregion were processed, and then parameters were adjusted to give an improved visual match with observed disturbance patterns. Once an approximate parameter set was established, the formal validation process described below was implemented. Images used for calibration were not used for validation.

It is recognized that this approach is somewhat subjective. An alternative would be to use the validation data as "training" to constrain and optimize the parameter selection for each ecoregion. Initially this approach was not use due to time constraints (the disturbance mapping needed to proceed in parallel with the validation data set creation) and because we wanted to maintain the independence of the validation data set to avoid circularity. However, in the future the training approach may be implemented in order to improve the disturbance data set.

5. Image-based validation and accuracy assessment

5.1. Reference data

The accuracy of the decadal LEDAPS disturbance maps has first been assessed through comparison with disturbance maps generated from dense (annual–biennial) time series of Landsat imagery. Through a related project (Goward et al., 2008), a stratified random selection of 23 Landsat scene centers has been generated across the United States (Fig. 4). The sampling methodology seeks to obtain a national random sample proportionally representative of forest types, with additional constraints to ensure geographic dispersion and preferential sampling for scenes with high proportions of forest cover (Kennedy et al., in preparation). A Landsat image time series has been assembled for each of these locations for the period 1985–2005 with either annual or biennial revisit frequency.

To generate the reference data set, three 15×15 km sub-windows were extracted from each image time series stack, and stand-clearing disturbance was assessed using semi-automated techniques (Fig. 4). For those image stacks west of the Great Plains, a team at Oregon State University performed an unsupervised classification of temporal spectral trajectories to identify disturbances. This involved the following steps:

1. Each multi-spectral image subset (atmospherically corrected through the LEDAPS/6S process) was converted to reflectance factor Tasseled-Cap wetness. The wetness images were then assembled into a multi-temporal (10-year) stack for each subset.
2. The 1992/2001 NLCD and digital orthoquads were used to assess the range (mean and standard deviation across time) of wetness values for stable (undisturbed) forests.

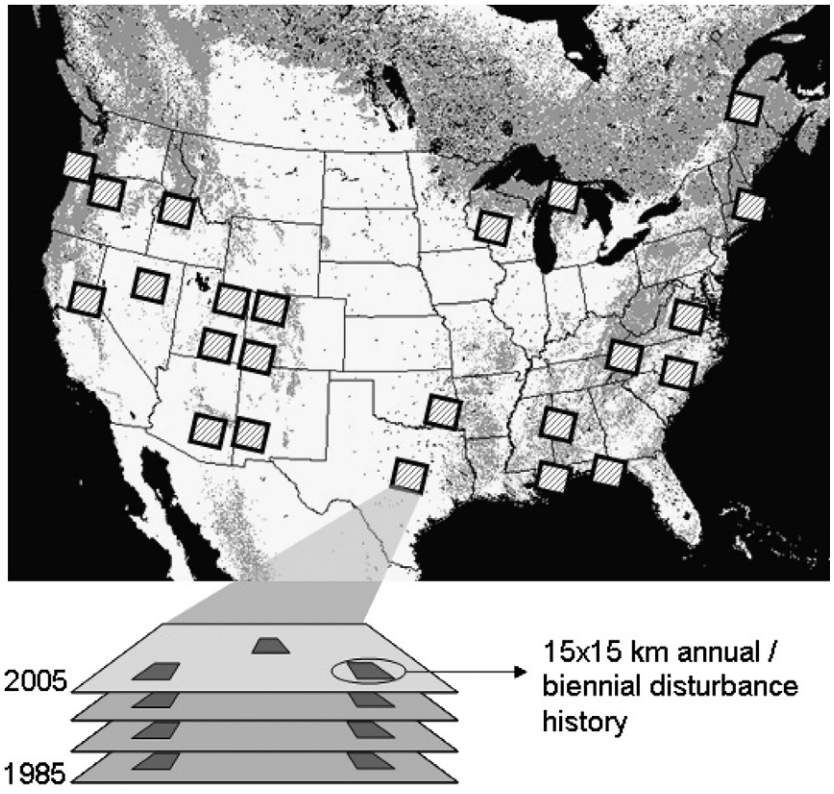

Fig. 4. Schematic illustration of validation data set preparation. The location of Landsat scenes used for validation in this study are shown superposed on map of IGBP forest cover derived from MODIS land-cover product. For each image time series, three 15×15 km subsets were randomly selected, and the per-pixel disturbance history was assessed for each.

3. An unsupervised technique (ISOCLUS) was used to identify 250 classes of temporal trajectories for each wetness stack.
4. These trajectories were evaluated manually to identify those matching major disturbance events in the imagery, and then used to map all disturbances within each stack.
5. Final results were sieve filtered (5-pixel kernel) to match the LEDAPS minimum-mapping area.

For image stacks from the eastern U.S. a team from University of Maryland used an approach based on spectral index thresholding. First, for each image in the stack, mature forest pixels were automatically identified using histogram thresholds (Huang et al., 2008). Then the mean ($\bar{b}$) and standard deviation (SD) of the spectral values of the identified forest pixels were used to calculate a forestness index (FI) value for each pixel in the concerned image:

$$\mathrm{FI} = \sqrt{\frac{1}{\mathrm{NB}}\sum_{i=1}^{\mathrm{NB}}\left(\frac{b_i - \overline{b}_i}{\mathrm{SD}_i}\right)^2} \quad (7)$$

where NB is the total number of spectral bands. Finally, for each pixel a temporal trajectory of the FI value was constructed using all images in a cube and forest disturbance was detected based on the shape FI trajectory. The final disturbance maps were then assessed visually against the original imagery to check the quality of the mapping.

The final reference data set includes disturbance maps for 69 15×15 km subsets extracted from 23 Landsat scene centers. Although two different approaches were used to develop the reference data set, both approaches (i) relied on dense time series of Landsat imagery; (ii) relied on hand editing and visual inspections of the results of an automated algorithm (hence they are "semi-automated"), and (iii) made use of higher resolution digital orthoquads and/or Quickbird imagery to resolve uncertainties in post-disturbance land-cover type. We acknowledge that the analysis performed here is not a full validation since we used Landsat imagery to assess the accuracy of a Landsat-based product. However, there is little doubt that large (stand-clearing) disturbance events are easily identified on annual to biennial Landsat time series (Cohen et al., 1998). While it would be ideal to be able to assemble time series of high-resolution air photos, which would allow counting of individual tree crowns through time, such data sets are not readily available through USGS or the National Archives. Instead we have opted to take advantage of the national sampling provided by the Landsat image stacks to provide a geographically comprehensive validation.

5.2. Multi-scale analyses

Several analyses were performed to cross-compare the LEDAPS results with the reference data sets. Pixel-level error matrices were prepared for each of the 69 subsets for the classes "disturbed" and "not disturbed" (null or cloudy pixels were excluded from the error matrix). Errors of omission and commission relative to the reference data sets were calculated from these matrices. Since the LEDAPS products are primarily targeted for regional carbon modeling studies, we have also quantified errors at coarser resolutions more appropriate for biogeochemical modeling. First, each 15×15 km reference subset was divided into 225 1-km resolution cells, and the total disturbed area within each cell was calculated and compared to the disturbed area within the corresponding LEDAPS product. Finally, an overall national analysis was performed by comparing the total disturbed area within each 15×15 km subset.

5.3. Statistical results

Fig. 5 shows the distribution of pixel-level errors (omission and commission) between the reference disturbance maps and the LEDAPS results for the class "disturbed 1990–2000". Twenty-nine

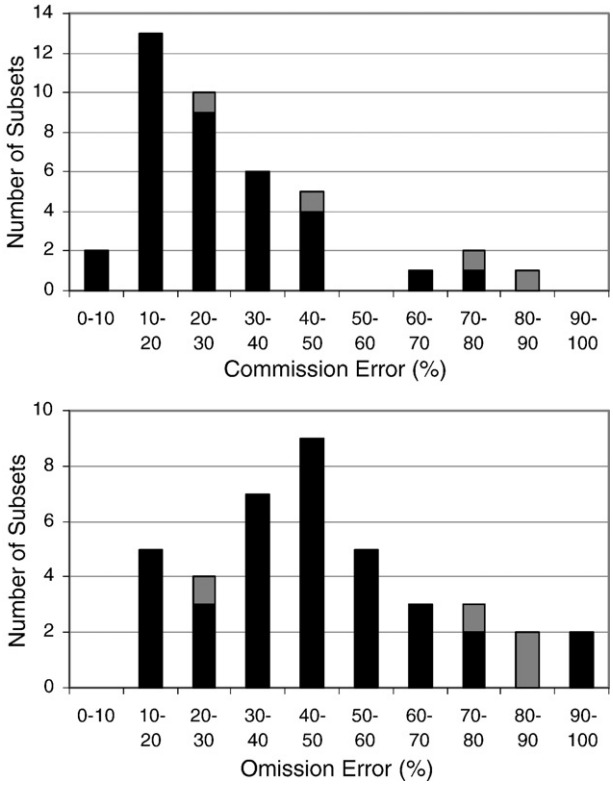

Fig. 5. The distribution of pixel-level errors of omission and commission for 40 15×15 km validation subsets from the random sample of US Worldwide Reference System (WRS-2) Landsat scenes (Fig. 4). Black bars correspond to subsets with >1000 pixels (0.4%) actual disturbance; grey bars correspond to subsets with <1000 pixels actual disturbance. An additional 16 subsets that had no observable disturbance are not shown here.

subsets with little or no observed disturbance in the reference data set (<100 pixels) have not been included since omission and commission errors are not meaningful for these sites. Errors of commission in the LEDAPS products (i.e. pixels mistakenly mapped as disturbance) are generally low, typically 10–30%, but errors of omission (i.e. actual disturbance not mapped) are much higher, typically 30–60%. A reasonable null hypothesis is that the DI algorithm has no spatial predictive power, in which case we would expect random agreement in proportion to the total amount of actual 1990–2000 disturbance mapped within the reference subsets. Since the average area disturbed in the reference data is 15% per decade, the null hypothesis would predict equal omission and commission errors centered on 85%.

Treating each 15×15 km subset as an independent sample from a normally distributed set of errors, we calculate a mean (national) omission error of 44.6 +/−5.8% and a mean commission error of 27.0 +/−4.5% where the uncertainties are calculated for 90% confidence interval using a two-sided test against the critical value of the *t*-distribution. This implies that LEDAPS is biased toward underestimating national disturbance by 17.6 +/−7.4%.

The higher errors of omission mostly reflect the limitations of using a decadal data set for mapping forest disturbance. As noted by other studies, the rate of forest regrowth can be sufficiently rapid to eliminate the spectral signal of disturbance within 10 years (Jin & Sader, 2005; Lunetta et al., 2004; Pussa et al., 2005; Steininger, 1996; Wulder et al., 2005). As a result, these stands are spectrally indistinguishable from older, mature stands, and are not detected as disturbance. The annual/biennial reference time series allows omission error to be calculated as a function of the time since disturbance. Most subsets show a systematic decrease in detection accuracy with time, indicating the difficulty in detecting disturbed stands after ~5 years of regrowth (Fig. 6). Considering just the most recent 2-year

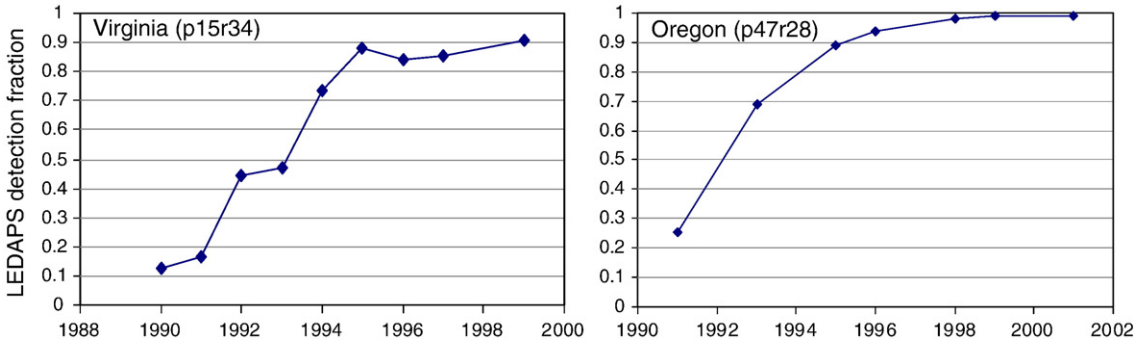

Fig. 6. Example of LEDAPS detection accuracy (1-omission error) as function of actual disturbance date for two 15×15 km subsets in Virgina (left) and Oregon (right). Disturbance date was determined with a precision of <2 years for reference data sets using the approaches described in the text. Detection accuracy of LEDAPS products drops for older disturbances, since regeneration masks the spectral signal by the end of the 10-year observation interval.

epoch (nominally 1998–2000) from six reference images from the Eastern U.S., the LEDAPS detection accuracy rises to an average of 74%.

The forest/non-forest masking is a secondary contributor to omission errors within LEDAPS. The fuzzy forest/non-forest classification has tended to underestimate forest cover slightly, causing some disturbances not to be mapped. Commission errors within LEDAPS are primarily due to misclassification of dense (deeply shadowed) agriculture as forest and occasional sensitivity of the algorithm to recent thinning. In addition, images that were acquired at widely separated parts of the seasonal growing cycle tend to exhibit high error rates. The ΔDI approach is self-normalizing, in that the Tasseled-Cap norming population (Eq. 2) comes from each image independently, and thus tends to resist small changes in BRDF and image phenology. However, when these changes become extreme (e.g. leaf-on vs. leaf-off seasonality), the ΔDI method breaks down.

To evaluate the performance of LEDAPS products at the 1-km scale, each 15×15 km reference subset was divided into 225 1 km cells, and the total area disturbed within each cell was compared to the LEDAPS product. We then calculated the linear (Pearson) correlation coefficient (R) between the reference and LEDAPS disturbance values (n=225 points) as:

$$R = \frac{\sum(x_i - \overline{x})(y_i - \overline{y})}{(n-1)\sigma_x\sigma_y} \quad (8)$$

where x_i is a single LEDAPS 1 km disturbance estimate, x is the mean LEDAPS disturbance estimate across all n=225 1-km cells, y_i and y are the comparable values for the reference data set, and σ_x and σ_y are the standard deviation of the LEDAPS and reference data sets, respectively. The distribution of R values among the 66 reference subsets is shown in Fig. 7, and most R values exceed 0.60.

At the coarsest scale of evaluation, Fig. 8 compares the LEDAPS estimates of disturbed area within each 15×15 km subset with the comparable value from the reference data set. The root mean squared error (RMSE) across the national sample is 566 ha out of a sample population of 22500 ha (i.e. the 15×15 km area). As is expected from the relatively higher omission errors in Fig. 5, most LEDAPS subsets show lower total disturbed area compared to the reference data set. It should also be noted that for many subsets "above" the 1:1 line (i.e. showing high rates of commission error), the additional disturbance mapped in LEDAPS were, in fact, "low magnitude" disturbances (such as thinning, partial harvests, or insect damage) flagged in the validation maps. While

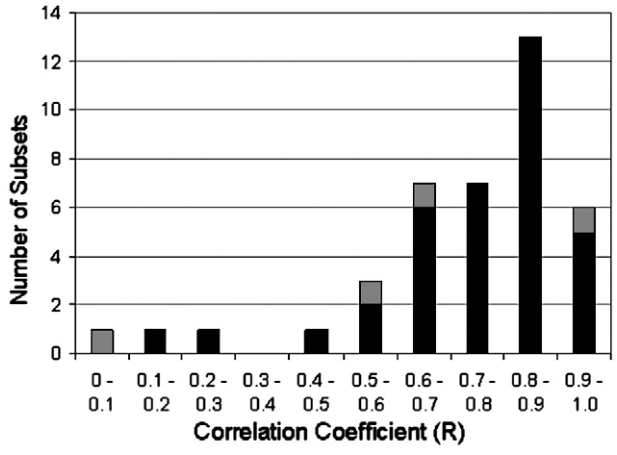

Fig. 7. Distribution of correlation coefficients (R) derived from calculating the area of disturbance within each 1 km cell in the LEDAPS and reference subsets. Black bars correspond to subsets with >1000 pixels (0.4%) actual disturbance; grey bars correspond to subsets with <1000 pixels actual disturbance. An additional 16 subsets that had no observable disturbance are not shown here. See text for discussion.

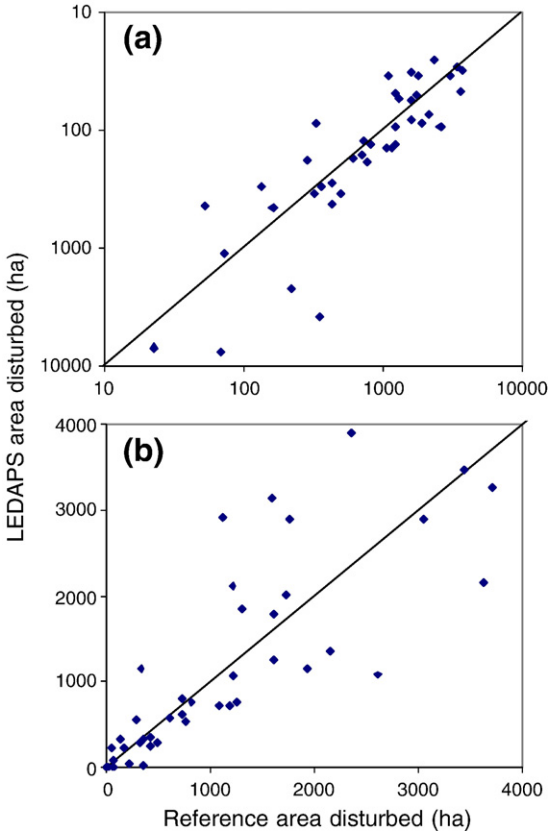

Fig. 8. Scatterplot of reference versus LEDAPS area disturbed within each 15×15 km subset (n=40), shown as (a) log–log and (b) linear plots.

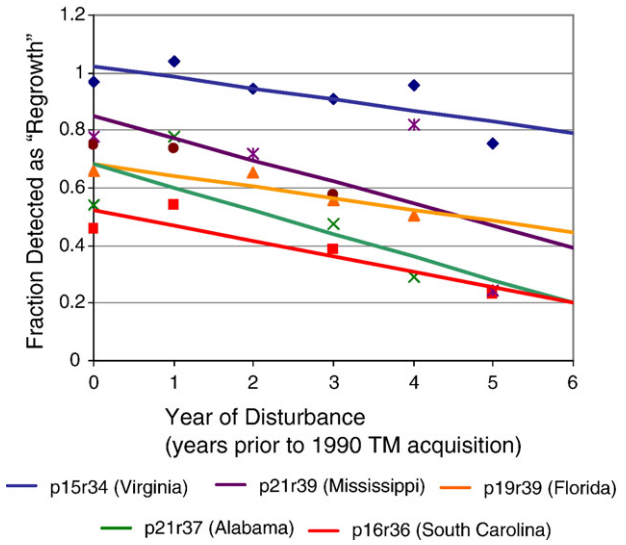

Fig. 9. Fraction of reference disturbances occurring in 1984–1990 that were mapped as "regrowth" by LEDAPS, as function of disturbance year, for five sites in the eastern United States.

these technically are commission errors, they are related to actual disturbance events and not simply spurious detections.

5.4. Regrowth detection capability

As noted in Section 2, the "regrowth" class must be calibrated to understand the sensitivity of the algorithm for detecting past disturbances that continued to accumulate biomass during the 1990–2000 observational period. In the future, we plan to assemble a longer time series of annual/biennial data for assessing disturbance events back to the 1970's using Landsat MSS. For now, however, we can use the existing reference data sets to examine the fraction of actual disturbances mapped for the 1984–1990 epoch that were detected by the LEDAPS regrowth class (Fig. 9). LEDAPS detects 50–100% of recently disturbed pixels as "regrowth". As expected the detection rate declines with the age of the disturbance. In general, the detection rate for disturbances of 5–6 years old is only half that of the most recent cohort. Given the limited ability to detect regrowth of older disturbances using the decadal data set, users must be cautious not to simply add the "disturbance" and "regrowth" figures for a particular location to obtain a net rate of change.

5.5. Visual comparisons

To illustrate the cumulative effect of omission and commission errors, it is useful to visually compare the LEDAPS and reference maps. Fig. 10 shows the reference disturbance map, the LEDAPS map, and the LEDAPS intermediate ΔDI product for two sites. The first, p47r28 in Oregon is an example with very low errors in omission and commission (12.9% and 13.7%, respectively), and as would be expected, there is excellent visual agreement between the reference and LEDAPS maps. The second case, p26r36 in Eastern Oklahoma yielded relatively poorer results, with higher errors of omission and commission (45.3% and 66.9%, respectively). Although much less spatially coherent, the patterns of disturbance and recovery also match the reference data set. The ΔDI map for Oklahoma is "noisier" compared to the Oregon site. This may reflect the wide seasonal gap between the 1990 and 2000 image for Oklahoma. The Landsat-5 image was acquired on July 8, 1990 while the Landsat-7 image was acquired on October 1, 2000.

6. Extension to continental scales

An initial set of processing parameters was generated for each CEC ecoregion, and the disturbance mapping algorithm was run on groups of contiguous scenes. Fig. 11 shows stand-clearing disturbance for 1990–2000 for the United States and Canada mapped using the LEDAPS approach. For this example, the 28.5-meter resolution change maps have been aggregated to 500–meter resolution representations of disturbance intensity by averaging the total disturbed area with each 500×500 m cell (excluding null areas such as clouds and shadow) and dividing by the non-null cell area.

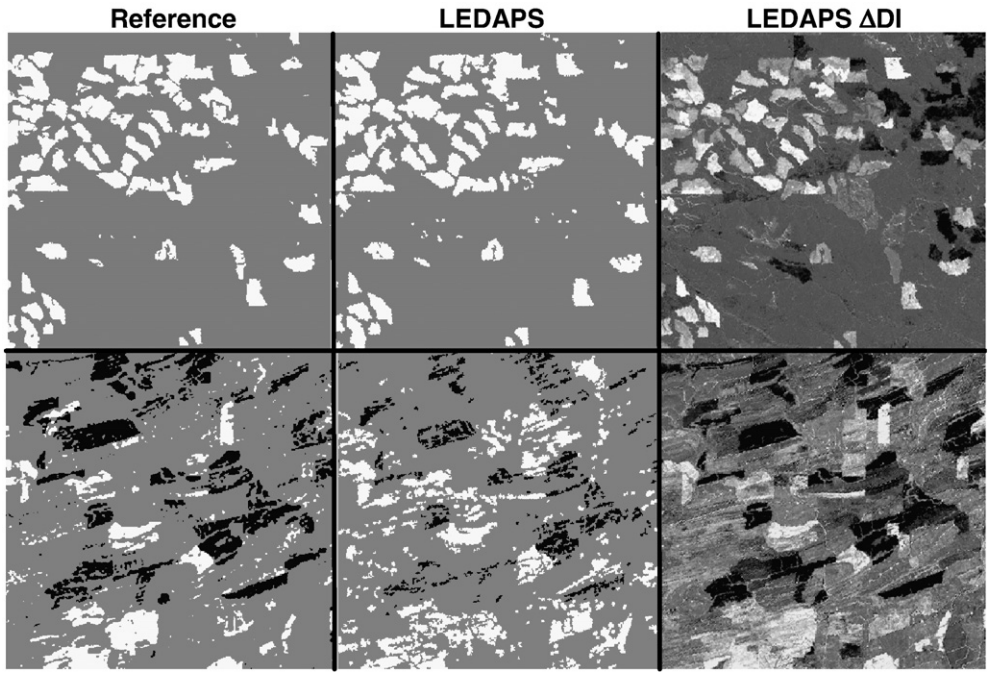

Fig. 10. Visual comparison of results from two 15×15 km subsets. Top row: p47r28 (Oregon); Bottom row: p26r36 (Eastern Oklahoma). Left: Reference disturbance data set (white = disturbed; black = regrowth); Middle: LEDAPS maps; Right: LEDAPS ΔDI arrays before thresholding. Higher values (bright areas) correspond to greater temporal change of the DI and biomass loss (disturbance). Note that the Oregon reference and LEDAPS maps do not include the regrowth class in this example.

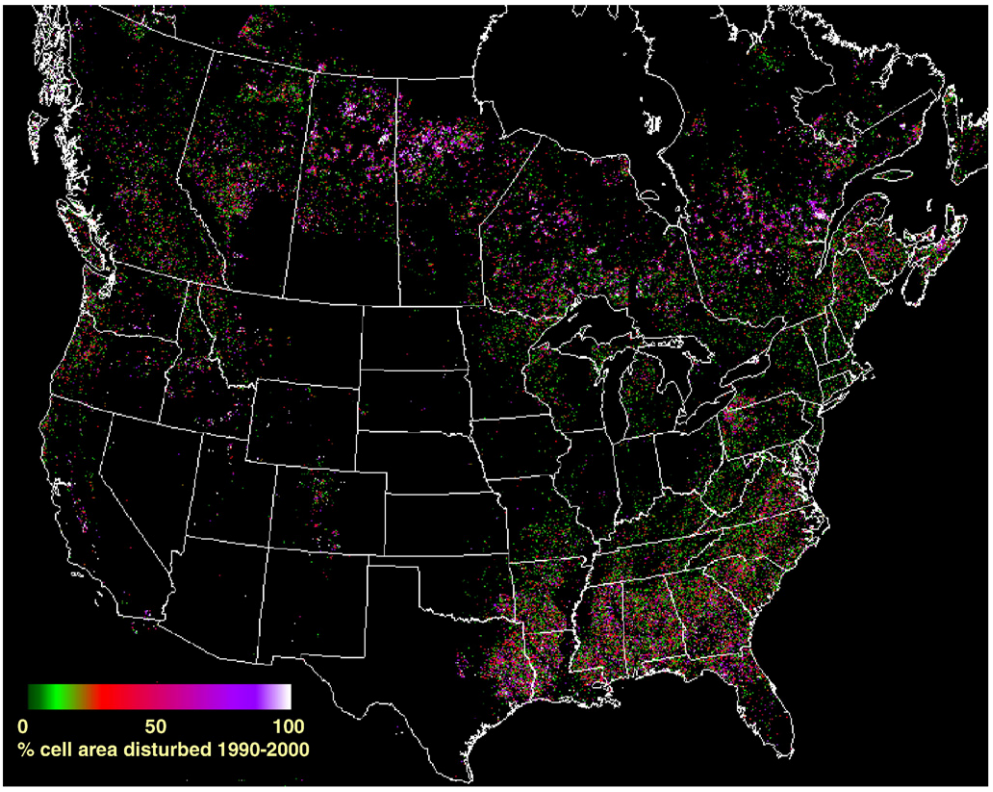

Fig. 11. Stand-clearing disturbance rates for conterminous United States and Canada, 1990–2000. Values are expressed in percent of 500×500 m cell area disturbed during the nominal 1990–2000 period.

The disturbance map illustrates broad patterns of forest dynamics across the continent. The boreal forests of Canada are dominated by large, discrete burn scars. Evaluating the mean disturbance rate across fire dominated portions of the central and eastern boreal region (Boreal Plains, Boreal Shield East, and Boreal Shield West ecozones) yields a total disturbed area of 8.47 million ha during the 1990s, or a rate of 0.41% of forest area per year. For comparison, Stocks et al. (2002) documented the area burned from 1959–1997 for the same regions and calculated a mean disturbance rate of 0.40% forest area burned per year. Given differences in methodology between this study and that of Stocks et al. (2002) the close agreement between the two rates may be regarded as partly coincidental. First, our estimate includes some contribution from logging and other disturbances as well as fire. Second, the Stocks et al. (2002) study only included large (>200 ha) fires, although large fires (>100 ha) are responsible for at least 99% of the area burned in the central Boreal forest (Larsen & MacDonald, 1998). It should also be noted that fire frequency appears to have increased since the 1970's. Using the most recent decade of data (1987–1997) from Stocks et al. (2002), the fire disturbance rate rises to 0.56% of forest area burned per year, somewhat higher than that calculated from the LEDAPS results.

The rate of 0.41% forest area per year corresponds to a fire frequency (mean return interval) of 244 years for the Boreal region of central Canada. Recent ecological studies have examined fire return interval in the Canadian Boreal forest using analysis stand age distribution, dendrochronology, and sediment cores (Bergeron et al., 2001; Carcaillet et al., 2001; Larsen & MacDonald, 1998; Larsen, 1997). Calculated return intervals vary considerably, from as low as 39 years for jack pine and aspen in Alberta (Larsen, 1997) to over 500 years for Holocene fires in Quebec (Carcaillet et al., 2001). In part, this reflects temporal variations in fire frequency throughout the Holocene. Bergeron et al. (2001) presented evidence for increasing fire return interval (decreasing frequency) in the Ontario and Quebec since the mid-19th century, which they attributed to long-term shifts in climate. Return intervals for the most recent epoch (1920–1999) fall into the general range of 191–521 years, similar to the results presented here and in Stocks et al. (2002), while those before 1850 tend to be much shorter (69–132 years).

Disturbance activity detected by LEDAPS in southern Canada and the conterminous United States is dominated by harvest activity rather than fire. Due to the limited sensitivity of LEDAPS to thinning and partia harvest, the LEDAPS maps primarily reflect the distribution of clearcuts. Mapped disturbance rates are highest in the southeastern United States, reflecting the prevalence of rapid rotation softwood forestry. The highest rates observed occur in northwestern Louisiana and eastern Texas where about 2.2% of the land area is cleared each year. From the validation study we may assume that the LEDAPS algorithm is underestimating disturbance by about 18% in this region. Applying this correction factor would suggest a rate of 2.6% per year, or a mean turnover period of 38 years. FIA data from the region indicate that about half the forestland area in northwestern Louisiana and eastern Texas is occupied by loblolly pine stands, and rotation periods of 20–25 years are typical for planted pine stands. Mean turnover periods for other forest types must be considerably higher (about 50–60 years) to produce the mean turnover period observed in the LEDAPS data.

Harvest rates are nearly as high in the Pacific Northwest, Maine, southern Quebec and parts of British Columbia. Like the southeastern United States these regions were sites of clearcut logging during the 1990's. Disturbance rates in the Mid-Atlantic, southern New England, and upper Midwest are significantly lower. In part this reflects differing management strategies in the northeastern United States. Forestry in this region is dominated by hardwood extraction, and relies on selective harvest of individual trees and techniques (e.g. strip cutting) that leave tree canopy intact (Smith & Darr, 2004). As a result we are probably underestimating the overall rate of harvest activity in the region.

Disturbance in the North American Cordillera follows a gradient of generally decreasing disturbance rates from north to south. The Canadian Rockies in Alberta and British Columbia are characterized by high rates of clearcutting and some fire activity. This pattern persists

into Montana and Idaho, but harvest activity becomes more limited in Colorado, Utah, and the southwestern United States. As discussed below, however, the ability of the LEDAPS algorithm to map disturbance in the sparse forests of the southern Rockies is limited.

Overall we estimate 21.7 million hectares of forest was disturbed in the conterminous United States (not including Alaska and Hawaii) during the 1990's. However, this figure can be adjusted for bias using the results from the validation study (Czaplewski, 1992). Knowing that the LEDAPS analysis fails to capture 18% of net disturbance (i.e. mean omission error − mean commission error), this figure should be increased to 25.6 million hectares. Estimates of the total forest cover of the continental United States vary. The US Forest Service FIA program estimated 251.1 million hectares of forestland based on a 10% stocking density threshold. In contrast, the MODIS VCF treecover product indicates 267 million hectares of land with greater than 20% tree canopy cover, and 335 million hectares of land with tree canopy cover greater than 10%. Taking the US Forest Service figure, we would conclude that 10.2% of US forest land was disturbed during the measurement interval. The mean measurement interval for this period is approximately 11 years (Table 1), corresponding to a mean forest turnover period of 110 years. For comparison, Smith and Darr (2004) estimate that clearcut harvest activities affected 1.50 million hectares of US forest each year, which would correspond to a mean rate of 5.9% of US forest cover on a decadal basis. It should be noted, however, that this estimate does not include effects of fire, which is included in the LEDAPS analysis.

The uncertainty associated with the national disturbance estimate depends on the uncertainty of the bias adjustment factor (18%): if there were no uncertainty about the omission and commission errors, the adjusted wall-to-wall disturbance estimate would be exact, In reality, the uncertainty in the bias adjustment comes from two factors: (i) the uncertainty about the calculated omission and commission errors, and (ii) the sampling error associated with selecting the validation sites themselves. The former error was estimated in Section 5.3 as +/−7.3%. The latter error is calculated as +/−17% (90% CI) knowing the mean disturbance rate from the validation sites and the fraction of US forest land sampled (Kennedy et al., in prep). Combining these factors, we estimate the overall uncertainty on the national disturbance estimate to be +/−24% at the 90% confidence level.

It might be argued that a more conservative error assessment would treat the individual validation scenes (rather than the 15 km subsets from within each scene) as independent samples, effectively reducing the number of samples. This assumption increases the error about the omission and commission errors to 9.6% and 8.8%, respectively, and increases the overall uncertainty for the national estimate to +/30%. In addition, this analysis assumes that the omission and commission errors follow a normal distribution. While this is approximately true (Fig. 5) it is also true that the mapping algorithm may fail entirely for a small number of individual scenes, leading to a relatively large number of “outliers” in the error distribution. Although we cannot provide an estimate for this effect, it does suggest that the calculated uncertainties could be somewhat higher.

7. Known issues and lessons learned

Not surprisingly, the DI algorithm has not performed equally well for all scenes in the North American GeoCover archive. In general the algorithm performs best for dark closed-canopy forests. A problematic region has been the southernmost Rockies and Intermountain West, dominated by pinyon pine, scrub oak, and juniper. The sparse treecover and low height of these forests results in background materials (grass, soil) contributing more to the overall spectral signal, and for the overall signal be easily confused with surrounding shrublands. In addition, the internal forest/non-forest masking has not yielded consistent scene-to-scene results in the northern boreal forest where, again, treecover is sparse and grades into shrub-, grass-, and moss-dominated landscapes. Although we anticipate improving the mapping for these regions, users of the initial LEDAPS products for these regions are encouraged to use the ΔDI fields directly in conjunction with locally-derived forest/non-forest masks.

About 20% of the GeoCover archive for North America is not directly usable for change detection because one or more images were acquired during senescent conditions. The only alternative in these cases has been to replace the GeoCover imagery with alternative scenes. The problem is particularly acute for eastern Canada, the Gulf Coast of the United States, and Mexico. In the latter case, almost none of the strongly dry-deciduous forests could be successfully mapped by LEDAPS because of the image acquisition dates and no products for Mexico are planned. A key recommendation from this project is that future assemblages of imagery for global change applications put a greater emphasis on inter-date compatibility and seasonality rather than achieving perfectly cloud-free coverage.

Our main focus in LEDAPS has been to map stand-clearing disturbance. However we also recognize that in so doing, we are missing a significant part of the timber extraction (and possibly carbon flux) from the continent. We may also introduce some regional bias into the continental maps. For example, during the 1980s and 1990s clearcutting accounted for ~26% of harvest area in the north-central and northeastern regions of the United States, but 44% of the area in the southern region (USFS FIA). Our maps will thus tend to underestimate the prevalence of disturbance in the former region.

Finally, it is clear from our results (e.g. Fig. 6) as well as previous studies that a 10-year repeat interval is not ideal for accurately mapping forest disturbance. The LEDAPS results tend to be biased towards the later part of the 1990s given the relatively poor detection capacity for older disturbance events. Previous studies have noted that an image refresh period of finer than 3–5 years is needed to map stand-clearing disturbance (e.g. Jin & Sader, 2005). It is reasonable to assume that some finer time interval (<2 years) is required for mapping more subtle disturbances that recover more rapidly, such as thinning or insect defoliation.

8. Conclusions

The LEDAPS project has mapped stand-clearing forest disturbance across North America during the 1990–2000 interval in support of the North American Carbon Program. Some 2200 Landsat GeoCover images have been processed using the Disturbance Index methodology of Healey et al. (2005). This paper has detailed the algorithmic basis for the LEDAPS mapping, and presented an image-based validation study of the results for the United States. Although the decadal revisit interval of the GeoCover data set is not optimal, the continental mapping captures the major patterns of stand-clearing disturbance in the United States and Canada. Calculated omission and commission errors generally range from 30–60% and 20–30%, respectively.

Disturbance rates vary widely across the continent. Fire dominates the disturbance regime of the Canadian boreal forest. The central boreal area burned during the 1990's mapping epoch corresponds to a mean turnover period of 240 years, in rough agreement with estimates from the ecological literature. Within the United States, the highest rates of disturbance are found in areas experiencing clearcut harvest practices, particularly the southeast, Maine, and the Pacific Northwest. Clearing rates in these areas reach 2–3% per year. The mean stand-clearing disturbance rate during the conterminous United States as a whole is calculated as 0.9 +/−0.2% per year, corresponding to a turnover period of 110 years. Although the uncertainty of this estimate is relatively large, and can be expected to be reduced in the future, this estimate represents the first wall-to-wall assessment of forest disturbance for the nation.

A related project (North American Forest Dynamics or NAFD; Goward et al., 2008) is currently mapping forest disturbance using a geographic sample of annual and biennial Landsat image time series.

The results from the NAFD project will complement those presented here by providing a more accurate estimate of disturbance rates and their variability through time, including non-clearing phenomena such as insect damage and thinning. In turn, the LEDAPS maps will support the extrapolation of NAFD results across the North American continent.

One of our goals has been to demonstrate automated approaches to mapping land-cover change that can be applied to continental-scale projects. Similar initiatives have been undertaken in Australia by the Australian Greenhouse Office and in Canada through the EOSD project (Wulder et al., 2003). International initiatives such as Global Observations of Forest Cover and Land Cover Dynamics (GOFC-GOLD) and national initiatives such as the Climate Change Science Program (CCSP) have specified the need for regular updates on land-cover and vegetation dynamics (including disturbance) at frequent (<5 year) intervals.

Critical to future monitoring of forest cover and disturbance is the ready availability of Landsat-like data. Landsat continuity has been difficult to ensure (Wulder et al., 2005), but multiple, international sources of data are now available from sensors such CBERS (China–Brazil Earth Resources Satellite) and the Indian Remote Sensing (IRS) Resourcesat-1. These resources also offer the prospect of improved temporal coverage for cloudy regions. In addition, the current schedule for the Landsat Data Continuity Mission (LDCM) promises a new source of Landsat data starting in 2011. Of equal importance, the USGS has announced plans to allow free distribution orthorectified data from the Landsat 1–7 archive beginning in 2009. These developments represent major advances for the land-cover research community, and should, for the first time, enable routine monitoring of forest dynamics around the globe.

Acknowledgements

This work was supported by grants from the NASA Terrestrial Ecology and Applied Sciences Programs. The comments from three anonymous reviewers substantially improved the manuscript. Sean Healey is thanked for his help with the Disturbance Index metric. Robert Kennedy and Stephen Stehman are thanked for the consultation regarding uncertainty analyses. Julia Barsi, Brian Markham, and Gaynesh Chander are thanked for assistance with the Landsat-5 calibration history.

References

Barford, C. C., Wofsy, S. C., Goulden, M. L., Munger, J. W., Pyle, E. H., Urbanski, S. P., et al. (2001). Factors controlling long- and short-term sequestration of atmospheric CO_2 in a mid-latitude forest. *Science*, *294*, 1688–1691.

Bergeron, Y., Gauthier, S., Kafka, V., Lefort, P., & Lesieur, D. (2001). Natural fire frequency for the eastern Canadian boreal forest: consequences for sustainable forestry. *Canadian Journal of Forest Research*, *31*, 384–391.

Carcaillet, C., Bergeron, Y., Richard, P. J. H., Frechette, B., Gauthier, S., & Prairie, Y. T. (2001). Change of fire frequency in the eastern Canadian boreal forests during the Holocene: does vegetation composition or climate trigger the fire regime? *Journal of Ecology*, *89*, 930–946.

Chander, G., Markham, B. L., & Barsi, J. A. (2007). Revised Landsat-5 thematic mapper radiometric calibration. *IEEE Geoscience and Remote Sensing Letters*, *4*, 490–494.

Commission for Environmental Cooperation (1997). *Ecological Regions of North America: Toward a Common Perspective, Montreal.* 60 pp.

Cohen, W. B., Fiorella, M., Gray, J., Helmer, E., & Anderson, K. (1998). An efficient and accurate method for mapping forest clearcuts in the Pacific Northwest using Landsat imagery. *Photogrammetric Engineering and Remote Sensing*, *64*, 293–300.

Cohen, W. B., & Goward, S. N. (2004). Landsat's role in ecological applications of remote sensing. *BioScience*, *54*, 535–545.

Cohen, W. B., Spies, T. A., Alig, R. J., Oetter, D. R., Maiersperger, T. K., & Fiorella, M. (2002). Characterizing 23 years (1972–95) of stand replacement disturbance in western Oregon forests with Landsat imagery. *Ecosystems*, *5*, 122–137.

Coppin, P., Jonckheere, I., Nackaerts, K., Muys, B., & Lambin, E. (2004). Digital change detection methods in ecosystem monitoring: a review. *International Journal of Remote Sensing*, *25*, 1565–1596.

Crist, E. P., & Cicone, R. C. (1984). Application of the Tasseled-Cap concept to simulated Thematic Mapper data. *Photogrammetric Engineering and Remote Sensing*, *50*, 343–352.

Crist, E. P. (1985). A TM tasseled cap equivalent transformation for reflectance factor data. *Remote Sensing of Environment*, *17*, 301–306.

Czaplewski, L. (1992). Misclassification bias in areal estimates. *Photogrammetric Engineering & Remote Sensing*, *58*, 189–192.

Goward, S. N., Masek, J. G., Cohen, W., Moisen, G., Collatz, G. J., Healey, S., et al. (2008). Forest disturbance and the North American carbon flux, EOS, Transactions. *American Geophysical Union*, *89*, 105–106.

Hansen, M. C., Defries, R., Townshend, J., Sohlberg, R., Dimiceli, C., & Carroll, M. (2002). Towards an operational MODIS continuous field of percent tree cover algorithm: examples using AVHRR and MODIS data. *Remote Sensing Environment*, *83*, 303–319.

Healey, S. P., Cohen, W. B., Zhiqiang, Y., & Krankina, O. N. (2005). Comparison of Tasseled-Cap-based Landsat data structures for use in forest disturbance detection. *Remote Sensing of the Environment*, *97*, 301–310.

Horler, D. N. H., & Ahern, F. J. (1986). Forestry information content of Thematic Mapper data. *International Journal of Remote Sensing*, *7*, 405–428.

Houghton, R. A. (1999). The annual net flux of carbon to the atmosphere from changes in land use 1850–1990. *Tellus Series B-Chemical And Physical Meteorology*, *51*, 298–313.

Huang, C., Wylie, B., Yang, L., Homer, C., & Zylstra, G. (2002). Derivation of a Tasseled-Cap transformation based on Landsat-7 at-satellite reflectance. *International Journal of Remote Sensing*, *23*, 1741–1748.

Huang, C., Song, K., Kim, S., Townshend, J., Davis, P., Masek, J., et al. (2008). Use of a dark object concept and support vector machines to automate forest cover change analysis. *Remote Sensing of Environment*, *112*, 970–985.

Jin, S., & Sader, S. A. (2005). Comparison of time-series tasseled cap wetness and the normalized difference moisture index in detecting forest disturbances. *Remote Sensing of Environment*, *94*, 364–372.

Kauth, R. J., & Thomas, G. S. (1976). The Tasseled-Cap — A graphic description of the spectral–temporal development of agricultural crops as seen by Landsat. *Proceedings, Symposium on Machine Processing of Remotely Sensed Data* (pp. 41–51). West Lafayette, IN: LARS.

Kennedy, R. E., Cohen, W. B., Moisen, G. G., Goward, S. N., Wulder, M. A., Powell, S. L., et al. (in preparation) A Landsat-based sampling design for estimating three decades of forest disturbance dynamics in the contiguous United States.

Kurz, W. A., & Apps, M. J. (1999). A 70-year retrospective analysis of carbon fluxes in the Canadian Forest Sector. *Ecological Applications*, *9*, 526–547.

Larsen, C. P. S. (1997). Spatial and temporal variations in boreal forest fire frequency in northern Alberta. *Journal of Biogeography*, *24*, 663–673.

Larsen, C. P. S., & MacDonald, G. M. (1998). Fire and vegetation dynamics in a jack pine and black spruce forest reconstructed using fossil pollen and charcoal. *Journal of Ecology*, *86*, 815–828.

Lobser, S. E., & Cohen, W. B. (2007). MODIS tasseled cap: Land cover characteristics expressed through transformed MODIS data. *International Journal of Remote Sensing*, *28*, 5079–5101.

Lu, D., Mausel, P., Brondizio, E., & Moran, E. (2004). Change detection techniques. *International Journal of Remote Sensing*, *25*, 2365–2407.

Lunetta, R. S., Johnson, D. M., Lyon, J. G., & Crotwell, J. (2004). Impacts of imagery temporal frequency on land-cover change detection monitoring. *Remote Sensing of the Environment*, *89*, 444–454.

Masek, J. G., & Collatz, G. J. (2006). Estimating forest carbon fluxes in a disturbed southeastern landscape: Integration of remote sensing, forest inventory, and biogeochemical modeling. *Journal of Geophysical Research*, *111*, G01006. doi:10.1029/2005JG000062

Masek, J. G., Vermote, E. F., Saleous, N., Wolfe, R., Hall, E. F., Huemmrich, F., et al. (2006). A Landsat surface reflectance data set for North America, 1990–2000. *Geoscience and Remote Sensing Letters*, *3*, 68–72.

Odum, E. P. (1969). The strategy of ecosystem development. *Science*, *164*, 262–270.

Pacala, S. W., Hurtt, G. C., Baker, D., Houghton, R. A., Birdsey, R. A., Heath, L., et al. (2001). Consistent land- and atmosphere-based US carbon sink estimates. *Science*, *292*, 2316–2320.

Pussa, K., Liira, J., & Peterson, U. (2005). The effects of successional age and forest site type on radiance of forest clear-cut communities. *Scandinavian Journal of Forest Research*, *20*, 79–87.

Reams, G. A., Smith, W. D., Hansen, M. H., Bechtold, W. A., Roesch, F. A., & Moisen, G. G. (2005). The forest inventory and analysis sampling frame. In W. A. Bechtold & P. L. Patterson (Eds.), *The Enhanced Forest Inventory and Analysis Program — National Sampling Design and Estimation Procedures. Southern Research Station General Technical Report SRS-80* (pp. 11–26). Asheville, NC: U.S. Department of Agriculture, Forest Service, Southern Research Station, 85 p.

Smith, W. B., & Darr, D. (2004). *US forest resource facts and historical trends.* US Department of Agriculture Publication FS-801 40 pp.

Steininger, M. K. (1996). Tropical secondary regrowth in the Amazon: Age, area and change estimation with Thematic Mapper data. *International Journal of Remote Sensing*, *17*, 9–27.

Stocks, B. J., Mason, J. A., Todd, J. B., Bosch, E. M., Wotton, B. M., Amiro, B. D., et al. (2002). *Large forest fires in Canada, 1959–1997J. Geophys. Res.*, *107*. (pp. 8149). doi:10.1029/2P001JD000484

Thornton, P. E., Law, B. E., Gholz, H. L., Clark, K. L., Falge, E., Ellsworth, D. S., et al. (2002). Modeling and measuring the effects of disturbance history and climate on carbon and water budgets in evergreeen needleleaf forests. *Agricultural and Forest Meteorology*, *113*, 185–222.

Tucker, C. J., Grant, D. M., & Dykstra, J. D. (2004). NASA's global orthorectified Landsat data set. *Photogrammetric Engineering and Remote Sensing*, *70*, 313–322.

Vermote, E. F., Vermote, E. F., El Saleous, N., Justice, C. O., Kaufman, Y. J., Privette, J. L., et al. (1997). Atmospheric correction of visible to middle-infrared EOS-MODIS data over land surfaces: Background, operational algorithm, and validation. *Journal of Geophysical Research*, *102*, 17131–17141.

Vogelmann, J. E., Howard, S. M., Yang, L., Larson, C. R., Wylie, B. K., & Van Driel, N. (2001). Completion of the 1990s National Land Cover data set for the conterminous United States from Landsat Thematic Mapper Data and ancillary data sources. *Photogrammetric Engineering and Remote Sensing*, *67*, 650–662.

Wickham, J. D., Stehman, S. V., Smith, J. H., & Yang, L. (2004). Thematic accuracy of the 1992 National Land-Cover data for the western United States. *Remote Sensing of the Environment*, *91*, 452–468.

Wofsy, S. C., & Harriss, R. C. (2002). *The North American Carbon Program (NACP).* Report of the NACP Committee of the U.S. Interagency Carbon Cycle Science Program Washington, DC: US Global Change Research Program.

Wulder, M. A., Dechka, J. A., Gillis, M. A., Luther, J. E., Hall, R. J., Beaudoin, A., et al. (2003). Operational mapping of the land cover of the forested area of Canada with Landsat data: EOSD land cover program. *Forestry Chronicle*, *79*, 1075–1083.

Wulder, M. A., Skakun, R. S., Dymond, C. C., Kurz, W. A., & White, J. C. (2005). Characterization of the diminishing accuracy in detecting forest insect damage over time. *Canadian J. Remote Sensing*, *31*.